

## Article

# Research on Seeding Performance of Self-Propelled Industrial Hemp Seeder

Yiping Duan <sup>1,2,†</sup>, Wei Xiang <sup>2,†</sup>, Jiangnan Lv <sup>2</sup>, Bo Yan <sup>2</sup>, Yao Hu <sup>2</sup> and Mingliang Wu <sup>1,\*</sup><sup>1</sup> College of Mechanical and Electrical Engineering, Hunan Agriculture University, Changsha 410128, China<sup>2</sup> Institute of Bast Fiber Crops, Chinese Academy of Agricultural Sciences, Changsha 410205, China

\* Correspondence: mlwu@hunau.edu.cn

† These authors contributed equally to this work.

**Abstract:** In order to solve the problems of high labor intensity and low production efficiency in the cultivation of hemp in hilly areas, the seed arrangement performance of self-propelled hemp seeders was studied. According to the cultivation mode of hemp for the fiber industry in Yunnan, Sichuan, and other hilly areas, the seed metering device for the hemp industry was designed, the seed metering mechanism of hemp was analyzed, and the theoretical value range of design parameters of its key components was determined. The row of kind of wheel speed is obtained by single factor experiment, hole diameter and hole depth and uniformity of the seed, the seed of change rule, on the basis of the quadratic regression orthogonal rotation combination test, two indexes of the regression model, using the regression model of the design parameter optimization, and seeder row of kind of verification test, the results show that: when the rotation speed of the metering wheel was 90.0 r/min, the diameter of the hole was 10.4 mm, and the depth of the hole was 6.4 mm, the coefficient of variation of seeding uniformity of seeding machine was less than 45%, and the coefficient of variation for consistency of seed quantity in each row was less than 8%. The operation of the self-walking industrial hemp seeder met the requirements of fiber industrial hemp planting in hilly areas.

**Keywords:** industrial hemp; seeder; metering device; experimental research



**Citation:** Duan, Y.; Xiang, W.; Lv, J.; Yan, B.; Hu, Y.; Wu, M. Research on Seeding Performance of Self-Propelled Industrial Hemp Seeder. *Appl. Sci.* **2022**, *12*, 8079. <https://doi.org/10.3390/app12168079>

Academic Editors: José Miguel Molina Martínez and Roberto Romaniello

Received: 22 June 2022

Accepted: 8 August 2022

Published: 12 August 2022

**Publisher's Note:** MDPI stays neutral with regard to jurisdictional claims in published maps and institutional affiliations.



**Copyright:** © 2022 by the authors. Licensee MDPI, Basel, Switzerland. This article is an open access article distributed under the terms and conditions of the Creative Commons Attribution (CC BY) license (<https://creativecommons.org/licenses/by/4.0/>).

## 1. Introduction

Industrial hemp is an annual non-toxic herbaceous plant belonging to Cannabaceae. It has no psychoactive and drug utilization value with a THC (tetrahydrocannabinol) content of less than 0.3%. Industrial hemp is rich in nutrients with high economic use value. It is mainly divided into fiber type, seed type, and medicinal type by usage, and is widely used in textile, food, medicine, health, daily chemical, and other fields [1,2]. According to statistics from China's Bureau of Statistics and the Food and Agriculture Organization of the United Nations, China has the world's largest industrial hemp cultivation area, accounting for about 50% of the world's total industrial hemp cultivation area. The industrial hemp industry is controlled by strict laws in China, and its legal cultivation area is mainly located in the Yunnan and Heilongjiang provinces of China. The mechanized planting area of industrial hemp is principally divided into the plain with vast territory and large seeding area, and the hills and mountains with little cultivated land and scattered seeding plots. The plain generally utilizes large-scale seeders or coating film seeders for work [3,4]. The hills and mountains generally utilize small and medium-sized seeders for work. Nevertheless, due to the lack of specialist industrial hemp seeders for fiber use, the planting of industrial hemp for use in fiber in hilly areas is still predominantly manual or semi-mechanical, as there is a lack of professional joint seeders for industrial hemp. The fibrous industrial hemp in the mountains and hills area is suitable for dwarf dense planting, and the main planting type is stripe sowing, with a total seeding quantity of 57.6~62.4 kg/hm<sup>2</sup>, row spacing of 150~250 mm, and sowing depth of 30~80 mm. The existing industrial hemp seeder

is mainly suspended, with large width and large turning radius. Consequently, it is not suitable for hilly and mountain operations, and the total seeding quantity does not meet the agronomic requirements [3–5]. Seeders are not only an essential element of the mechanized planting of industrial hemp but also an inevitable way to propel the production efficiency of industrial hemp [6,7]. It is urgent to develop a self-propelled seeder suitable for planting fiber industrial hemp in mountains and hills areas.

The seed metering device is the core part of the seeder. An efficient and reliable seeder is the key to ensuring the working quality and efficiency of the seeder [8–10]. According to the working principle, the seed metering device is divided into mechanical and pneumatic types [11–13]. Pneumatic seed metering devices have good adaptability to seeds, high precision of single seed metering, and low seed damage rate. Nevertheless, its complex structure, high energy consumption, and easy sealing can be affected by machine vibration, leading to strict requirements for the working environment. The mechanical seed metering device has the advantages of simple structures, strong versatility, and easy to achieve dense seeding [14–16], which has become the first choice for mechanized seeding of hemp for the fiber industry in hilly and mountainous areas. The fiber industrial hemp shape ellipse, small particle size, lightweight, researchers worldwide have conducted numerous studies on small size seed metering devices. For instance, Wang et al. [17] designed a central roller seed arrangement device to address the common problems of high damage rate and low seeding accuracy in the rice seeding process, researched the influence of roller speed on seed arrangement performance, and improved the applicability to different seeds by replacing rollers with shaped holes. To meet the requirements of high speed and precision seeding of corn seeder, according to the material characteristics of flat corn seeds, Liu et al. [18] designed a horizontal disc metering device with an inclined longitudinal rectangular hole to make the metering plate. With this device, the forward chamfer and side chamfer produced vertical force on the seeds, which slowed down the time for the seeds to leave the metering plate and improved the metering performance. İbrahim Ethem Güler et al. [19] researched the influences of shaped hole diameter, actual working length, and rotational speed on the filling rate and seeding uniformity of the alfalfa seed metering device. The results indicated that the seeding performance is better when the diameter of the hole, the working length of the metering wheel, and the rotational speed of the metering wheel are 6.0~8.0 mm, 15.0~25.0 mm, and 20.0~40.0 r/min, respectively. Singh, R.C. et al. [20] researched the influence of cone taper of seed tray-type holes on seeding quality. As indicated from the results, the missed seeding index and replay seeding index was 1.3% and 4%, respectively, when the seeding disc velocity, vacuum degree, and cone angle were 0.42 m/s, 2 kPa, and 120°. Arzu Yazgi et al. [21] researched the effects of seed metering devices with different numbers of holes on cotton and maize seeding plate. Singh et al. [22] used electronic control metering system to monitor and give feedback on the seeding process of the precision metering devices in real-time, which reduced the miss-seeding rate and improved the seeding quality.

As revealed from the mentioned research, optimizing the hole structure of seed metering devices improves seed filling and seed metering performance effectively. Mechanized planting technology for small grain crops such as rice and maize has mainly been mature. However, research on industrial hemp seeding devices is extremely rare. In this paper, according to the technical requirements of industrial hemp planting. A self-propelled industrial hemp seeder was designed. The structure, working principle, and key components of the seeder were introduced. We studied the design parameters of the rotational speed of the metering wheel, the hole diameter, and the hole depth, and identified these as the main influencing factors of our hypothesis. We then carried out the parameter optimization test.

## 2. Structural Principle and Design Requirements

### 2.1. Structure of Machine and Seed Metering Device

As shown in Figure 1a, the self-propelled industrial hemp seeder was mainly composed of a Dynamic chassis system, Seeding and fertilizing system, Ditch seeding system,

and control systems. The matching power of the seeder is 6.3 kW, the weight of the whole machine is 350 kg, the breadth is 1.1 m, it can sow 3~6 rows, the seed depth is 30~80 mm, it can open the trench 3~6 rows, the working speed is 2~5 km/h, the total of seeding quantity is 57.6~62.4 kg/hm<sup>2</sup>, Fertilizer application rate is 50~125 kg/hm<sup>2</sup>, rear-wheel drive seeding operation, compact machine structure, light and compact weight, small turning radius, can complete the furrowing, sowing, fertilization, and other processes.

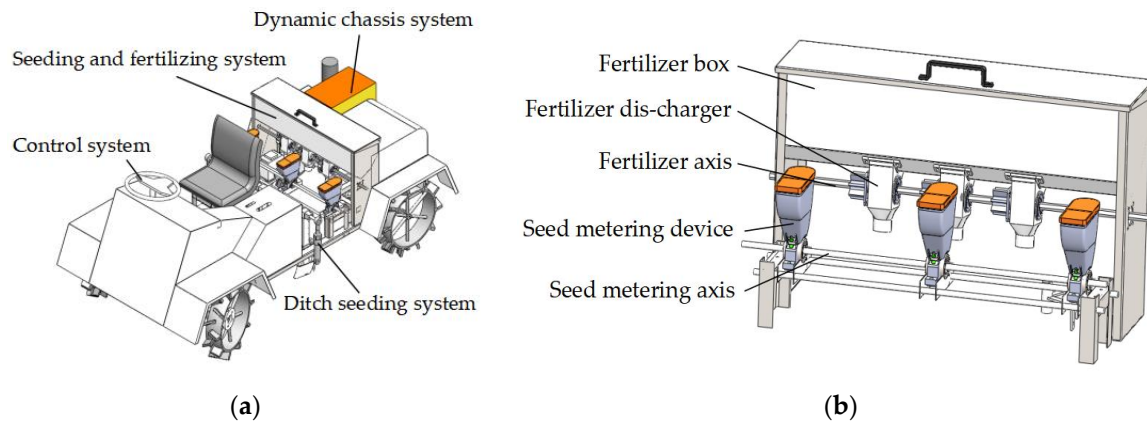


**Figure 1.** Self-propelled industrial hemp seeder. (a) Whole structure (b) Seeding and fertilizing system.

Figure 1b shows the metering and fertilization system of the self-propelled industrial hemp seeder, mainly composed of a fertilizer box, fertilizer applicator, seed applicator, fertilizer applicator shaft, and seed applicator wheel. The power is input into the metering and fertilization system through the power chassis system to drive the seed applicator and fertilizer applicator to work and realize the seeding function. According to the agronomic requirements of the hemp fiber industry in mountainous areas, the metering mechanism adopts the hole wheel metering device, which can install 3~6 metering devices. Each metering device is installed parallel through the metering shaft, convenient for adjusting the row spacing. The seed metering shaft and fertilizer metering shaft are chain transmissions to ensure synchronous seed metering and fertilization operation.

As the core component of the metering and fertilization system, the working performance of the metering device directly determines the working quality of the seeder. The type hole wheel seed metering device mainly comprises a box cover, seed box, flexible baffle, inoculation cup, seed cleaning brush, seed protector, and seed metering wheel, as shown in Figure 2. There are several shaped holes in the radial direction of the metering wheel that are concentrically coordinated with the metering shaft. The brush and seed protection plate connect with the shell thread through the nut.

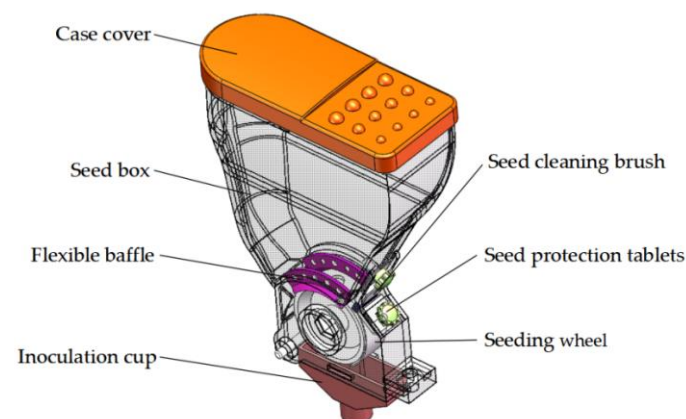


**Figure 2.** Type hole wheel seed metering device.

### 2.2. Seeding Mechanism

When the seed metering device works, the seeds mainly pass through the four sections of the filling area I, clearing area II, protecting area III, and throwing area IV, as shown in Figure 3. The power is driven by the transmission system’s input metering shaft to drive the metering wheel’s rotation. The seeds in the seed box gradually form a dynamic circulating seed group from the aggregation static state driven by the metering wheel. Under the combined action of gravity, metering wheel friction, and side seed pressure, the seeds are ‘scooped’ from the hole’s edge into the hole to complete the filling. The seeds of industrial hemp encapsulated in the hole were rotated along with the rowing wheel. When the seeds were rotated to the brush with the roller, the brush and the rowing wheel would row the seeds back to the seed box through mutual friction to complete the seed cleaning. Then the seeds left in the hole continued to rotate with the metering wheel under the protection of the seed plate and rotated to the falling point to fall under the action of gravity to complete the protection and seeding.

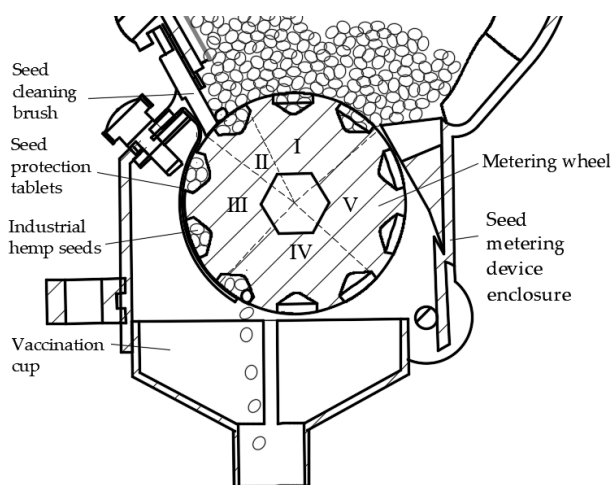


Figure 3. Operation process of seed metering device.

### 2.3. Metering Quantity Requirement

Whether the seeding quantity can meet the requirements of industrial hemp planting is the key to the design of the seeder. Referring to ‘Hemp crop production machinery’ [23], to meet the requirements of fiber industry hemp planting in hilly and mountainous areas, the self-propelled industrial hemp seeder must be strip-seeded. The amount of fiber industry hemp planting needs to reach 57.6~62.4 kg/hm<sup>2</sup>, and the working efficiency is above 60.0 hm<sup>2</sup>/h. Based on the operating width of the seeder being 1.1 m, the operating speed is 4.7 km/h, and seeding three rows at a time, the walking distance of the machine operation 1.0 hm<sup>2</sup> is about 9.1 km. The corresponding seed rate *q* and total seeding quantity *Q* should meet the Formula (1), and the seed rate *q* is 165.3~179.1 g/min.

$$\begin{cases} t = \frac{L_b}{v_b} \\ Q = 3qt \end{cases} \quad (1)$$

where *L<sub>b</sub>* is the moving distance of 1.0 hm<sup>2</sup> of machinery operation, km; *t* is the time required for the machine to move 1.0 hm<sup>2</sup>, h; *q* is the amount of seed metering device, g/min; *Q* is total seeding quantity, kg/hm<sup>2</sup>; *v<sub>b</sub>* is the operating speed of the machine, km/h.

## 3. Parameter Design and Analysis of Critical Components of Seed Metering Device

### 3.1. Basic Parameters of Industrial Hemp Seeds

As the basic parameters of industrial hemp seeds, triaxial size, and the three-dimensional size of the seed are important references for designing the shape and size of the hole [24–26].

Among them, the 1000-seed weight is an important index to measure the seed quantity of the seed metering device, which refers to the absolute quality of 1000 industrial hemp seeds without impurity and damage. Therefore, industrial hemp seeds' shape, size, 1000-grain weight, and moisture content were determined.

In this study, "Long Ma 3" belongs to the main fiber-based promotion product in China, and the self-propelled industrial hemp seeder needs to realize the precision seeding of fiber-based industrial hemp. Therefore, we choose "Long Ma 3" as the research object, and in order to minimize the adverse effects of different sizes of seeds on the operation of the seeder, we selected 100 seeds to measure their length, width, and thickness and repeated them five times. The electronic balance and moisture content tester measured the seeds' 1000-grain weight and moisture content. The average 1000-grain weight and moisture content were obtained through five repeated experiments. The results indicated that the seed shape of "Long Ma 3" was approximately elliptical, the average moisture content was 7.6%, and the average thousand-seed weight was 15.1 g. The coefficient of variation of length, width, and thickness were 1.3%, 1.2%, and 1.0%, respectively. The size difference between seed materials is microscopic. Table 1 shows the measurement results.

**Table 1.** Three axis sizes of industrial hemp seed.

Parameter	Mean Value/mm	Maximum Value/mm	Coefficient of Variation/%
Length	3.9	4.2	1.3
Width	3.0	3.2	1.2
Thickness	2.4	2.5	1.0

### 3.2. Parameter Design of the Metering Wheel

The design mainly includes the diameter and thickness of the metering wheel, the shape, diameter, depth, the number of holes, and the rotation speed of the metering wheel [27]. Figure 4 shows the schematic diagram of the metering wheel structure. The structure of the hole-wheel seed metering device on the market was measured as a reference, and the thickness of the seed metering wheel were designed to be 20.0 mm.

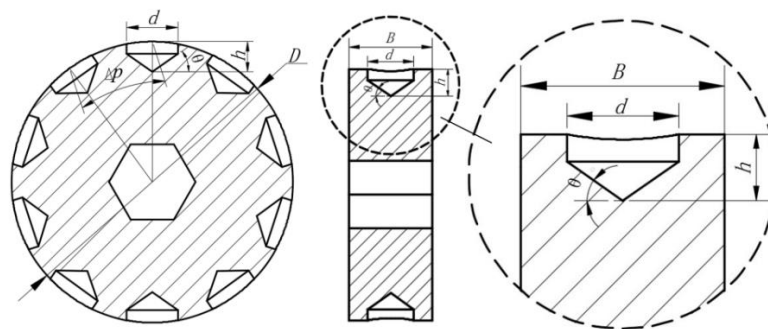


**Figure 4.** Structure of metering wheel. Note:  $D$  is the diameter of the metering wheel, mm;  $h$  is the hole depth, mm;  $\theta$  is the cone angle of the hole, °;  $\Delta p$  is the distance between adjacent holes, mm;  $B$  is the thickness of metering wheel, mm.

#### 3.2.1. Diameter of Metering Wheel

The diameter of the metering wheel is the primary structural parameter of the metering device, which determines the structural distribution of the metering device and the structural size of other components [28]. It is an essential factor affecting the filling performance. The diameter of the metering wheel should meet the following formula.

$$\begin{cases} v_n = \pi D n \\ \pi D = Z \Delta p \end{cases} \quad (2)$$



where  $v_n$  is the line speed of the metering wheel, m/s;  $d$  is the diameter of the metering wheel, mm;  $n$  is the rotational speed of the metering wheel, and r/min;  $z$  is the number of circular holes.

It can be seen from Formula (2) that under certain conditions, the larger the diameter of the metering wheel is, the longer the seed retention time in the seed filling area, and the more the number of holes can be increased to improve the filling quality. However, when the rotation speed of the metering wheel is constant, the larger the diameter of the metering wheel is, the greater the linear velocity is. When the linear velocity exceeds the relative velocity of the filling limit, it will affect the filling quality. Reducing the diameter of the metering wheel can reduce the linear velocity of the metering wheel but making it too small will lead to an increase in the curvature of the metering wheel and reduce the seed filling efficiency [29]. Therefore, referring to the current research results of the hole metering device and combining it with the previous test results, the diameter of the seed row wheel is 40.0~60.0 mm.

### 3.2.2. Hole Design

The seed length of “Long Ma 3” is greater than the width, and the width is greater than the thickness. According to the minimum potential energy principle, the seed is more likely to be encapsulated into the hole in a “flat” posture [30,31]. Considering that “Long Ma 3” is elliptical, it is convenient for the seed to fall out of the hole smoothly. The designed hole is cone-shaped, and the cone angle of the hole is 45°. To ensure that the hole of the metering wheel can fill more seeds at one time, the diameter of the hole should be at least two seeds at the same time. The hole diameter should be greater than the sum of the maximum length of the industrial hemp seed and the maximum width of the seed and less than two-thirds of the thickness of the metering wheel. The structural strength of the metering wheel should be ensured to prevent damage to the metering wheel at high speeds and affect the metering performance. The hole depth should be satisfied so that the multi-seeds can fully enter the hole in the overlapping state. Considering the posture of the seed being encapsulated into the hole, the hole height should be twice the maximum thickness of the seed. The hole diameter and depth should meet Formula (3) [32].

$$\begin{cases} (L_{\max} + H_{\max}) \leq d \leq \frac{2}{3}B \\ (L_{\max} + w_{\max}) \leq d \leq \frac{2}{3}B \\ 2H_{\max} \leq h \\ h < d \end{cases} \quad (3)$$

where  $L_{\max}$  is the maximum length of industrial hemp seed, mm;  $h_{\max}$  is the maximum seed thickness of industrial hemp, mm;  $w_{\max}$  is the maximum seed width of industrial hemp, mm.

The maximum length, width, and thickness of the “Long Ma 3” seed were 4.1 mm, 3.2 mm, and 2.5 mm, respectively. Comprehensive formula, the hole’s diameter, and depth should meet  $6.7 \text{ mm} \leq d \leq 13.0 \text{ mm}$  and  $h \geq 5.0 \text{ mm}$ .

$$\Delta p \geq 2L_{\max} \quad (4)$$

According to the maximum seed length of 4.1 mm, the distance between the holes should be greater than 8.2 mm. The general plant spacing of industrial hemp strip seeding is 10.0 mm, and the linear speed of the hole wheel is generally not more than 0.3 m/s. The operating speed of the known seeder is 4.7 km/h, and the number of holes meets the Formulas (5) and (6) [33].

$$Z = \frac{\pi d v_b}{S v_n} \quad (5)$$

$$v_\omega = \omega D \quad (6)$$

where  $S$  is the theoretical spacing, mm;  $\omega$  is the angular velocity of the metering wheel, rad/s,  $v_\omega$  is the linear velocity of the metering wheel, m/s.

Combined with the Formulas (2) and (4)–(6), the number of holes in the metering wheel is  $8.8 \leq Z \leq 17.9$ , and the angle between adjacent holes is taken as integral as possible to facilitate processing. The number of holes in the metering device is designed to be 10.

### 3.2.3. Speed of Seeding Wheel

The filling effect of the seed metering device directly affects its seeding performance. Whether the seed falls into the hole smoothly depends on the relative motion between the seed and the metering wheel. The speed of the metering wheel will affect the filling effect. The seed filling process is a dynamic system consisting of the gravity of the seed itself, the inter-species force, the positive pressure between the seed and the metering wheel, the sliding friction force, and the rolling friction force. It is a complex process to separate the seed from the population. In order to obtain the theoretical value range of speed of the seed metering wheel, the expanded kinematic analysis of the seed filling process is shown in Figure 5.

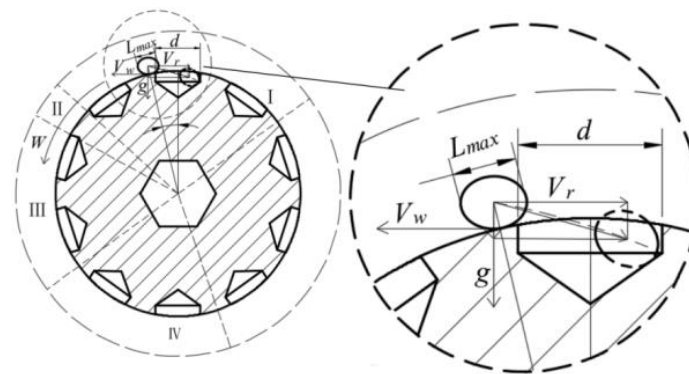


**Figure 5.** Kinematic analysis diagram of seed filling into the shaped hole. Note:  $v_r$  is the ultimate relative velocity of the seed successfully entering the shape hole, m/s;  $L_{max}$  is the maximum length of the seed, mm;  $g$  is the acceleration of gravity, m/s.

The Formulas (7) and (8) should be satisfied between the hole’s limit relative velocity and the rotational speed when the seed is in the X-axis’s transverse direction and the Y-axis’s vertical direction [32].

$$v_\omega = v_r \left( d - \frac{L_{max}}{2} \right) \sqrt{\frac{g}{L_{max}}} \tag{7}$$

$$\omega = \frac{2\pi n}{60} \tag{8}$$

Comprehensive Formulas (6)–(8) The value formula of the rotational speed of the metering wheel (9)

$$n \leq \frac{30}{\pi R} \left( \left( d - \frac{L_{max}}{2} \right) \sqrt{\frac{g}{L_{max}}} \right) \tag{9}$$

where  $n$  is the rotational speed of the metering wheel, r/min;  $r$  is the radius of the metering wheel, mm.

The diameter of the metering wheel was 60.0 mm, the diameter of the hole was  $6.7 \text{ mm} \leq d \leq 13.0 \text{ mm}$ , and the maximum length of the seed was 4.2 mm, which was substituted into Formula (9) to obtain  $69.7 \text{ r/min} \leq n \leq 155.1 \text{ r/min}$ .

### 3.2.4. Seed Cleaning Process Analysis

Seed cleaning is the premise to ensure the precision of seed arrangement. The industrial hemp seeds in the holes are cleaned out by brush to ensure the number of holes filled

into the seeds. When more than two seeds were filled, the seeds could not be filled entirely into the hole. A small part of the seeds was filled into the hole, and most of them were exposed outside. Then the seed cleaning was completed under the impact of the cleaning brush. The cleaning process is simplified to facilitate the force analysis of the seed cleaning process [34]. In the theoretical analysis of the cleaning process, it is assumed that the impact force of the cleaning brush on the seed is a single force, and the friction force between the seed and the hole wall is negligible. The following mechanical model was established.

Figure 6 shows the cleaning process. When a seed passes through the filling area and reaches the cleaning area, the seed is unstable and falls back to the filling area under the impact of the flexible brush. The seeds are jointly affected by the centrifugal  $F_n$  and friction  $f$  of the seeds in the hole, the extrusion force  $F_1$  of the population, the impact force  $F_C$  of cleaning seeds, and the gravity  $G_1$  of the seeds themselves. The condition for the seeds to leave the hole under the scouring force of the brush is as follows: under a certain angular velocity, the seeds need to leave the population for discrete motion. A rectangular coordinate system centered on the centroid of the seed is established. and the equilibrium equation of seed force is as follows

$$\begin{cases} F_C \cos \beta_1 \geq f \cos \gamma_1 \\ F_C \sin \beta_1 + F_n \cos \gamma_1 + m\omega^2 R \cos \gamma_1 \geq G_1 + F_1 \cos \gamma_1 \end{cases} \quad (10)$$

where  $F_C$  is seed cleaning impact force, N;  $\beta_1$  is the angle between the  $x$ -axis direction and the brush impact force, N;  $\gamma_1$  is the clearing angle, ( $^\circ$ );  $m$ , average 1000-grain weight of seeds, g;  $g_1$  is the population resultant force of seeds during seed cleaning, N;  $f_n$  is the centrifugal force on seeds during seed conservation, N;  $f$  is interspecies friction, N;  $f_1$  is extrusion force, N.

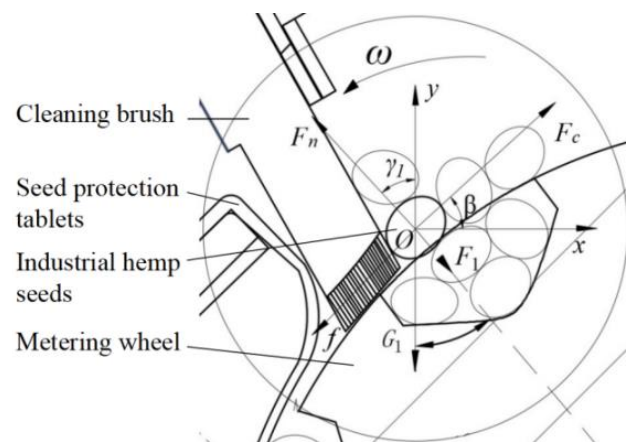


Figure 6. Seed cleaning process analysis.

Comprehensive Formula (10):

$$F_C \geq G_1 + \left( \frac{F - m\omega^2 R - F_n - f}{\cos \gamma_1} \right) \quad (11)$$

It can be seen from Equation (11) that under the premise of ensuring the reliability of seed cleaning, when the centrifugal force, friction force  $f$  and support force  $F_n$  of seeds are constant, the larger the population extrusion force and the smaller the included angle, the greater the seed cleaning impact force  $F_C$ . The larger the angle between the two types of holes is, the greater the  $\gamma_1$  is, that is, the smaller the seed cleaning force is, so the angle between the type holes should not be too large.



### 3.2.5. Analysis of the Process of Seed Protection and Seed Arrangement

In order to reasonably design the diameter of the seeding wheel and avoid the phenomenon of carrying seeds, feeding seeds, and rubbing seeds between the hole and the seed protection chip in the process of seed protection, ensure the stability of seed transportation in the process of seed protection, and analyze the stress of the seeds in the process of seed protection. Figure 7 shows the process of seed protection.

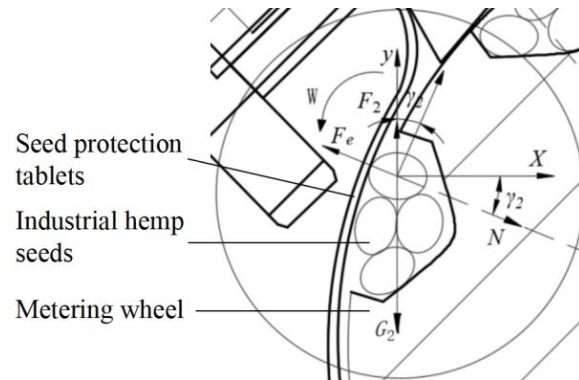


Figure 7. Analysis of seed protection process.

A specific lateral seed in the hole was taken as the research object to facilitate the theoretical analysis of the seed protection process. If the radial resultant force acting on the seed in the hole were less than the centrifugal force, the seed would produce a movement trend from the bottom to the outside, making the seed contact with the seed protection chip. It was easily damaged by the friction force generated by the seed protection plate on the seed. Therefore, the force of the seed in the seed protection process should meet the formula:

$$\begin{cases} \sum F_y = 0, & G_2 \cos \gamma_2 + F_2 - F_e = 0 \\ \sum F_x = 0, & G_2 \sin \gamma_2 - F_2 = 0 \\ F_2 = f \cdot N \cos \gamma_2 \\ F_e = mr\omega^2 \\ G_2 = mg \end{cases} \quad (12)$$

where  $G_2$  is the gravity of the seed in the process of conservation,  $N$ ;  $\gamma_2$  is the seed protection angle, ( $^\circ$ );  $f_2$  is the resultant force of interaction force between seeds during seed protection,  $N$ ;  $F_e$  is the centrifugal force of seeds during seed protection,  $N$  is the normal reaction,  $N$ ;  $r$  The distance between the centroid of the seed and the center of the runner, mm.

From Formula (12):

$$\omega = \sqrt{\frac{g(\cos \gamma_2 + \sin \gamma_2)}{r}} \quad (13)$$

The results showed that when the protecting angle  $\gamma_2$  was constant, the smaller the diameter of the seed row wheel was, that is, the smaller the distance from the centroid of the seed to the circular rotation center of the shaped hole was, and the larger the angular velocity of the seed row wheel was, the greater the effect of the seed guard plate on the seed was. In order to reduce seed breakage, the diameter of the seed row wheel should be increased.

To further explore the influence of seed row wheel diameter on seed row, the seed row process was analyzed, as shown in Figure 8. The type of hole cannot arrange seeds smoothly, which will directly affect the precision of the seed metering device and cause uneven seed metering. In order to determine the conditions of seed arrangement, the stress analysis was carried out in the process of seed arrangement.

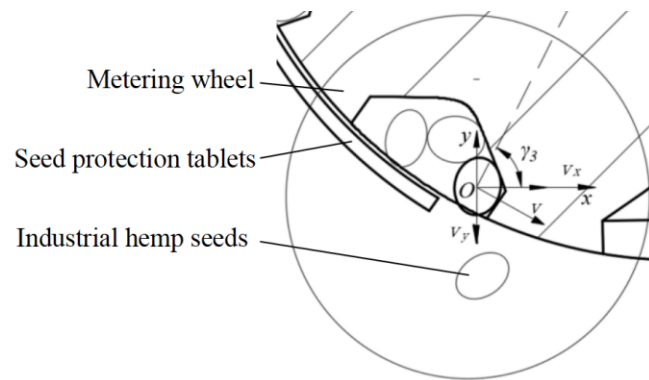


Figure 8. Analysis of seeding process.

The seeds fall under the action of centrifugal force and gravity. The seed group in the hole is regarded as a rigid whole, and its geometric center is its centroid. The  $xOy$  rectangular coordinate system is established. Assuming that the interaction between seeds is ignored during seeding, the plane velocity can be decomposed into the horizontal velocity  $v_x$  and the vertical downward velocity  $v_y$ , and the seed trajectory equation is obtained as follows [35]:

$$\begin{cases} X = v_x t \\ Y = v_y t + \frac{gt^2}{2} \\ V_x = v \cdot \sin \gamma_3 \\ v_y = v \cdot \cos \gamma_3 \\ V = \frac{n\pi R}{30} \end{cases} \quad (14)$$

where  $X$  is horizontal displacement, mm;  $v_x$  is the horizontal component of seeding speed, m/s;  $t$  for seeding time, s;  $y$  is the displacement in the vertical direction, mm;  $v_y$  is the vertical component of seeding speed, m/s;  $\gamma_3$  is the seeding angle, ( $^\circ$ );  $v$  is seeding speed, m/s.

From Formula (14):

$$\begin{cases} X = \frac{n\pi R \sin \gamma_3 t}{30} \\ Y = \frac{n\pi R \cos \gamma_3 t}{30} + \frac{gt^2}{2} \end{cases} \quad (15)$$

To prevent the seeds from a collision with each other when the seeds are entirely separated from the hole in the hole and fall from the adjacent hole, it is necessary to meet the below formula.

$$\begin{cases} \frac{\pi n R \cos \gamma_3 t_1}{30} + \frac{gt_1^2}{2} > R - R \cos \partial \\ \partial = \frac{\pi n R}{30} \end{cases} \quad (16)$$

In the formula:  $\gamma_3$  is the seed angle, ( $^\circ$ );  $t_1$  is the time of seed detachment, s;  $\partial$  is the rotation angle of the metering wheel after the seed is detached from the hole, ( $^\circ$ ).

According to the analysis of the seed arrangement process, when the structural parameters of the seed arrangement wheel are constant, the speed of the seed arrangement wheel can be appropriately increased in order to reduce the time for the seed to leave the shaped hole; when the rotation speed of the seeding wheel is constant, the time of seed escaping from the shaped hole is related to the seeding angle. To some extent, the larger the seeding angle is, the larger the diameter of the shaped hole is, and the time of seed escaping from the shaped hole is relatively smaller. Therefore, based on the analysis of the process of seed protection and seeding, the designed seed row diameter is 60.0 mm.

Based on the above analysis, referring to the number of holes of seed row wheel type  $8.8 \leq Z \leq 17.9$ , considering the convenience of processing adjacent holes, the included angle

should be rounded as far as possible. The number of holes of seed row type is 10, and the included angle of the two holes is  $36^\circ$ . The rotation speed, hole depth, and hole diameter of the seed row wheel should meet the requirements of  $69.7 \text{ r/min} \leq N \leq 155.1 \text{ r/min}$ ,  $6.7 \text{ mm} \leq d \leq 13.0 \text{ mm}$ , and  $h \geq 5.0 \text{ mm}$ , respectively.

#### 4. Test and Verification of Seed Metering Device

##### 4.1. Test Purpose

The rotational speed of the metering wheel, the depth of the hole, and the diameter of the hole are necessary conditions to ensure the quality of the metering. Referring to the relevant industry standards of performance test of the seeder, the bench test of the industrial hemp seeder was carried out with the rotational speed of the metering wheel, the depth of the hole, and the diameter of the hole as the test factors, and the seeding amount and the uniformity of the row as the test indexes. The multi-factor test was carried out to obtain the optimal parameter group of the seed metering device to explore the influence of these three factors on the uniformity of seed metering and the consistency of each row. The verification test was conducted to test whether the self-propelled industrial hemp seeder meets the agronomic requirements of fiber industrial hemp planting.

##### 4.2. Test Equipment and Materials

Main equipment: JPS-12 seeding performance test bench; scale (range 3 m, precision 1 mm); vernier caliper (range 150 mm, accuracy 0.1 mm); steel ruler (measuring range 200 cm, accuracy 1 mm); cup (500 mL); dT-2235A rotational speed instrument (accuracy 0.01 r/min); hX2002T electronic balance scale (weighing range 2000 g); each camera, computer, and timer.

The bench test was conducted in the Agricultural Mechanization Engineering Training Center of Hunan Agricultural University, Choose the “Long Ma 3” (Institute of Bast Fiber Crops, Chinese Academy of Agricultural Sciences, Changsha, China) as test seeds. The test bed primarily comprises a JPS-12 seeding performance test bed, control table, and hole wheel metering device. The plate-fixed metering device is used in the seeding performance test bed. Figure 9 shows the test devices. The control panel tested the operation parameters such as the rotation speed of the metering wheel, the conveying speed of the seedbed belt, and the oil flow rate.

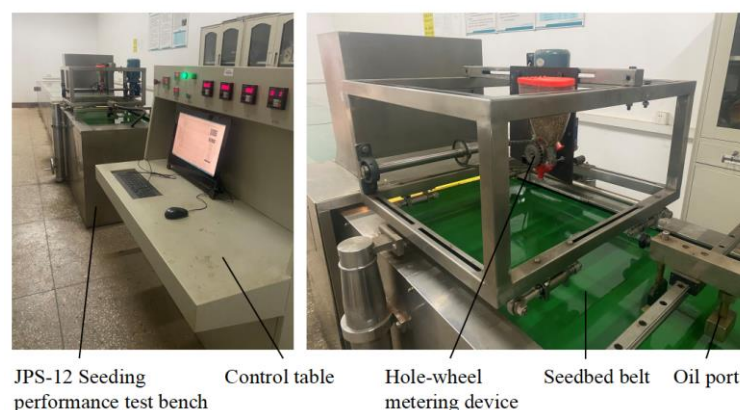


**Figure 9.** JPS-12 Seeding performance test bench.

##### 4.2.1. Parameter Optimization Test

According to ‘GBT 9478-2005 Test Method for Grain Strip Planter’ [36] the design of the hole wheel metering device was taken as the test object. The single factor test was carried out with the rotational speed of the metering wheel, the hole’s depth, and the hole’s diameter as the test factors, and the variation coefficient of the uniformity of the metering and the metering amount as the test indexes. The influence of various factors on the metering performance of industrial hemp was sought. As mentioned in Section 2.2, the parameter

design results were  $6.7 \text{ mm} \leq d \leq 13.0 \text{ mm}$ ,  $h = 5.0 \text{ mm}$ ,  $69.7 \text{ r/min} \leq n \leq 155.1 \text{ r/min}$ , and the operating speed of the seeder was set as  $4.7 \text{ km/h}$ , the rotational speed of the metering wheel was designed as  $70.0\sim 110.0 \text{ r/min}$ , the diameter of the hole was  $9.0\sim 13.0 \text{ mm}$ , and the depth of the hole was  $4.5\sim 8.5 \text{ mm}$ . Three groups of horizontal tests were repeated. In the experiment,  $5.0 \text{ m}$  on the conveyor belt of the test bench was taken as the measurement section, and the number of seeds in the ten groups of  $0.5 \text{ m}$  long areas was randomly counted to obtain the variation coefficient of seeding uniformity. The seed metering amount was obtained by measuring the average quality of the seeds rowed for  $1 \text{ min}$  when the seed metering device worked steadily.

#### 4.2.2. Parameter Optimization Test

After the single factor test, the influence relationship between rotation speed, hole diameter, and hole depth on seed row quantity and variation coefficient of seed row uniformity was obtained, and the value range of experimental factors in the multi-factor test was obtained under the premise that the total of seeding quantity was  $57.6\sim 62.4 \text{ kg/hm}^2$ . The seeding device's optimal structural and working parameters were obtained to further explore the influence of the interaction of various factors on the seeding device's performance. The rotation speed of metering wheel  $X_1$ , the diameter of hole  $X_2$  and the depth of hole  $X_3$  were taken as the test factors, and the variation coefficient of seeding uniformity  $Y_1$  and the coefficient of variation for consistency of seed quantity in each row  $Y_2$  were taken as the evaluation indexes for the multi-factor test. The coefficient of variation for consistency of seed quantity in each row was randomly selected  $5 \text{ m}$  as the test area, and the quality of each line of industrial hemp seeds was obtained to calculate the coefficient of variation for consistency of seed quantity in each row in the test area. The ternary quadratic orthogonal rotation combination test was used, and the data processing and statistical analysis were carried out by Design-Expert 11.0 software. The optimal parameter group of the seed metering device was obtained, and the performance verification test of the self-propelled industrial hemp seeder was carried out.

#### 4.3. Evaluation Indicators

According to the national standard 'GB9478-2005 test method of grain strip planter,' the variation coefficient of seeding uniformity and the coefficient of consistency of each row were selected as evaluation indexes. Seeding uniformity measures the uniformity of the seed's longitudinal distribution in the row, which needs to be less than or equal to  $45.0\%$ . Formula (19) shows its calculation. The coefficient of variation for consistency of seed quantity in each row's displacement refers to the consistency degree of each row's displacement under the same conditions. It is the main index to measure the quality of crop field distribution, which should be less than or equal to  $8\%$ , as shown in Formula (22). To a certain extent, the smaller the variation coefficient of seeding uniformity and the coefficient of variation for consistency of seed quantity in each row, the better the seeding performance of the metering device.

$$\bar{Z} = \frac{\sum Z_i}{N} \quad (17)$$

$$S_{Z_i} = \sqrt{\frac{\sum (Z_i - \bar{Z})^2}{N - 1}} \quad (18)$$

$$C_v = S_{Z_i} / \bar{Z} \times 100\% \quad (19)$$

where  $\bar{Z}$  is average number of seeds per segment;  $Z_i$  is the number of seeds per segment;  $S_{Z_i}$  is the standard deviation;  $N$  is the total number of segments, taking  $10$ ;  $C_v$  is the variation coefficient for seeding uniformity, %.

$$\bar{q}_i = \frac{\sum q_i}{n} \quad (20)$$

$$S_{q_i} = \sqrt{\frac{\sum(q_i - \bar{q})^2}{n - 1}} \tag{21}$$

$$\alpha_i = S_{q_i} / \bar{q} \times 100\% \tag{22}$$

where  $\bar{q}_i$  is average number of seeds per row;  $q_i$  is the number of seeds per row;  $S_d$  is the standard deviation;  $n$  is the number of rows, take 3;  $\alpha_i$  is the consistency coefficient for each row, %.

#### 4.4. Single Factor Test Results

##### 4.4.1. Effect of the Rotational Speed of the Metering Wheel on Each Index

Figure 10 shows the single-factor test results of the influence of the rotation speed of the metering wheel on seeding performance. The results showed that when the hole diameter was 11 mm and the hole depth was 6.5 mm, the variation coefficient of seeding uniformity decreased first and then increased with the increase in rotational speed of the metering wheel. The seed metering quantity increased with the rise of the rotation speed of the metering wheel. The seed metering quantity was 152.22~176.01 g/min at the rotation speed of 80~100 r/min, which met the seed metering quantity index of 150.10~178.29 g/min.

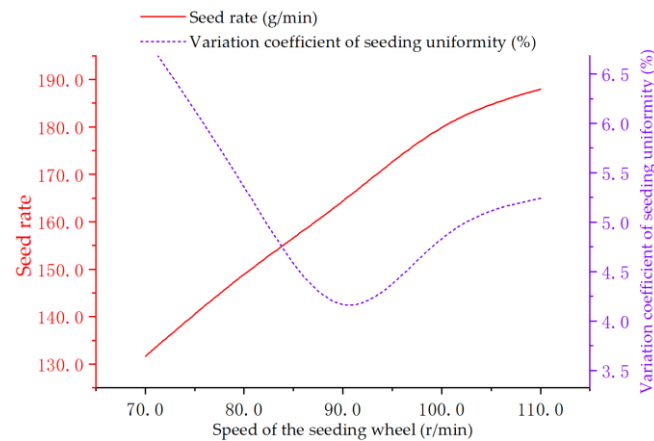


Figure 10. Relationship curve between the rotational speed of the seeding shaft and each index.

When the rotation speed of the metering wheel is low, the stirring effect of the metering wheel on the seed is poor, which leads to the seed being still in the accumulation state and cannot be separated from the seed pile. The irregular movement between populations is small, and the probability of the seed filling the hole is reduced, resulting in leakage and uneven distribution of seeds. When the rotation speed of the metering wheel is too large, the disturbance of the metering wheel on the flow layer of the population is substantial. It lead to the seeding before the number of seed filling in a single pore reaches the standard, leading to the problem of missing seeding. The high-speed rotation of the metering wheel causes the amplitude of the metering device to become more extensive, and the seeds are prone to offset when falling to the conveyor belt, which affects the uniformity of seed distribution. Therefore, the appropriate rotation speed of the metering wheel can effectively improve seeding performance.

##### 4.4.2. Effect of Hole Diameter on Each Index

Figure 11 shows the single factor test results of the effect of hole diameter on seeding performance. The results showed that when the rotational speed of the metering wheel was 90 mm and the depth of the hole was 6.5 mm, the variation coefficient of seeding uniformity decreased first and then increased with the increase in the hole diameter. The seed metering quantity increased with the increase in the rotational speed of the metering wheel. The seed rate of 10~12 mm hole diameter was 150.95~177.34 g/min, which met the seed rate index of 150.10~178.29 g/min.



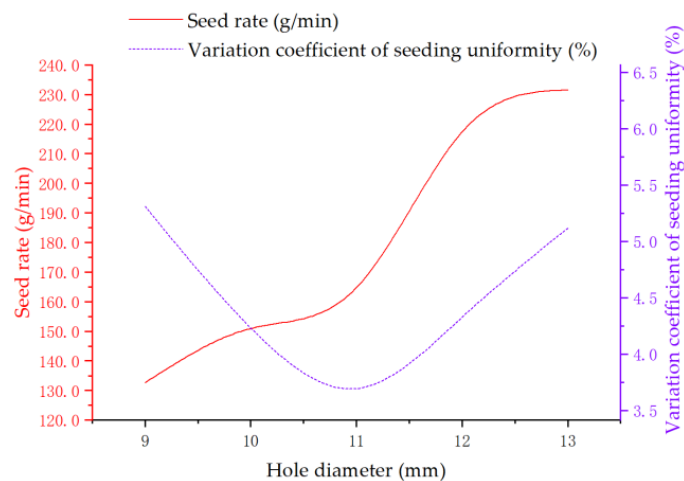


**Figure 11.** Relationship curve between hole diameter and indexes.

The reason is that the hole diameter is too small, and the seeds are filled with ‘vertical posture’ in the filling process. The probability of incomplete seed filling into the hole increases, resulting in a decrease in the number of seed filling and uneven distribution of seeds. If the diameter of the hole is too large, the seed is easier to fill the hole and the seed metering capacity increases. Still, some seeds with significant differences in particle size make the filling number of a single hole unstable and affect the metering performance. Therefore, the hole diameter has a significant impact on the seeding effect.

#### 4.4.3. Effect of Hole Depth on Each Index

Figure 12 shows the single-factor test results of the effect of hole depth on the seeding performance. The results showed that when the rotation speed of the metering wheel was 90 r/min and the diameter of the hole was 11 mm, the variation coefficient of seeding uniformity decreased first and then increased with the increase in depth. The seed rate increased with the increase in rotation speed. The seed rate of 5.5~7.5 mm hole depth was 143.62~178.09 g/min, which met the seed rate index of 150.10~178.29 g/min.

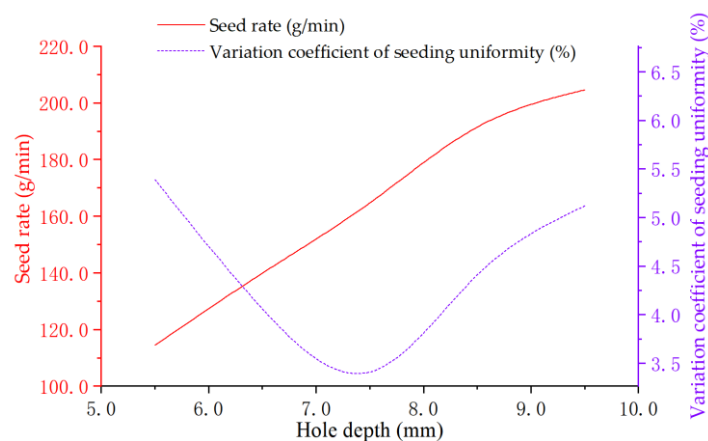


**Figure 12.** Relationship curve between hole depth and each index.

When the hole depth is too tiny, large particles of seeds are not filled by the hole, causing seeds to be brushed back to the filling area, resulting in filling instability. When the depth of the hole is too large, the time for seeds to fall out of the hole is prolonged, which may lead to seeds in the hole failing to unload. The seeds in the hole are returned to the filling area with the rotation of the metering wheel, which affects the subsequent seeding operation and the seeding performance. Therefore, the hole depth has a significant influence on the seeding effect.

Combined with the single factor test results, when the operating speed of the machine is 4.7 km/h, the rotational speed of the metering wheel is 80~100 r/min, the diameter of the hole is 10~12 mm, and the depth of the hole is 5.5~7.5 mm, the variation coefficient of the uniformity of the metering device is the minimum. The seed rate is 150.1~178.3 g/min. Therefore, the rotational speed of the metering wheel is 80~100 r/min, the hole diameter is 10~12 mm, and the hole depth is 5.5~7.5 mm.

#### 4.5. Multi-Factor Test

##### 4.5.1. Test Results and Regression Model Establishment

Combined with the results of single-factor research, the multi-factor test was carried out with the rotation speed of the metering wheel 80~100 r/min, the diameter of hole 10~12 mm, and the depth of hole 5.5~7.5 mm as the horizontal range to study further the influence of various factors on the working performance of seed metering devices. Table 2 shows the horizontal coding table of test factors.

Table 2. Coding with factors and levels.

Coding	Factor		
	Speed of Metering Wheel $x_1/(r \cdot \min^{-1})$	Hole Diameter $x_2/\text{mm}$	Hole Depth $x_3/\text{mm}$
-1	80.0	10.0	5.5
0	90.0	11.0	6.5
1	100.0	12.0	7.5

The multivariate nonlinear regression models of the variation coefficient  $Y_1$  of seeding uniformity and the consistency coefficient  $Y_2$  of each row with respect to the rotational speed  $x_1$  of the metering wheel, the diameter  $x_2$  of the profiled hole, and the depth  $x_3$  of the profiled hole were established using Design-Expert 11.0 software. The models and coefficients are tested. Table 3 shows the test scheme and results.

Table 3. Protocols and results.

Experimental Number	Experimental Factor			Experimental Index	
	Speed of Metering Wheel $x_1$	Hole Diameter $x_2$	Hole Depth $x_3$	Variation Coefficient of Seeding Uniformity $Y_1/\%$	Coefficient of Variation for Consistency of Seed Quantity in Each Row $Y_2/\%$
1	-1	0	1	5.78	2.03
2	0	-1	-1	5.73	1.22
3	1	0	-1	6.12	1.14
4	-1	-1	0	5.11	2.09
5	0	0	0	3.45	0.69
6	0	0	0	3.64	0.81
7	-1	0	-1	6.13	1.29
8	1	-1	0	6.43	0.89
9	1	0	1	6.55	1.06
10	0	0	0	3.78	0.76
11	0	1	1	5.67	1.67
12	-1	1	0	6.22	1.51
13	0	0	0	3.61	0.81
14	0	1	-1	5.59	1.05
15	0	0	0	3.69	0.89
16	1	1	0	6.07	1.73
17	0	-1	1	4.82	1.19

Note:  $x_1$  and  $x_2$ , and  $x_3$  indicated the levels value of Speed of metering wheel, Hole diameter, and Hole depth, respectively. The same is below.

(1) The regression equation of variation coefficient  $Y_1$  of seeding uniformity is:

$$Y_1 = 3.63 + 0.20x_1 + 0.18x_2 - 0.25x_3 - 0.37x_1x_2 + 0.34x_1x_3 + 0.26x_2x_3 + 1.62x_1^2 + 0.70x_2^2 + 1.13x_3^2 \tag{23}$$

Table 4 was the result of the variance analysis. The regression model of variation coefficient of row uniformity showed that the model was extremely significant ( $p < 0.01$ ) and the model was effective ( $p > 0.05$ ). determination coefficient  $R^2 = 0.991$ ; the calibration determination coefficient was 0.979, both close to 1, and  $CV = 3.12\%$ , accuracy Adeq precious = 82.66, indicating that the fitting equation has high reliability. Among them, the rotational speed of the metering wheel and the depth of the hole have a very significant indigenous effect on the equation. The diameter of the hole has a considerably indigenous effect on the equation. The influence of various factors on the variation coefficient of seeding uniformity is in the order of the rotational speed of the metering wheel  $x_1 >$  the depth of the hole  $x_3 >$  the diameter of the hole  $x_2$ . From the Formula (23), the variation coefficient of seeding uniformity  $Y_1$  and the rotational speed of metering wheel  $x_1$ , the diameter of the hole  $x_2$ , and the depth of the hole  $x_3$  showed the quadratic function of opening upward, respectively. It showed an optimal parameter combination of the rotational speed of the metering wheel, the diameter of the hole, and the hole depth, which made the variation coefficient of seeding uniformity minimum.

**Table 4.** Variation coefficient of seeding uniformity analysis results.

Variance Source	Variation Coefficient of Seeding Uniformity $Y_1/\%$				
	Sum of Square	Degree of Freedom	Mean Square	F Value	p Value
Model	20.12	9	2.24	85.23	<0.0001 **
$x_1$	0.47	1	0.47	17.75	0.0048 **
$x_2$	0.27	1	0.27	10.16	0.0090 *
$x_3$	0.07	1	0.07	2.68	0.0014 **
$x_1 \times 2$	0.54	1	0.54	20.59	0.0012 **
$x_1 \times 3$	0.15	1	0.15	5.80	0.0019 *
$x_2 \times 3$	0.25	1	0.25	9.34	0.0074 *
$x_1^2$	9.58	1	9.58	364.97	<0.0001 **
$x_2^2$	2.80	1	2.80	106.73	<0.0001 *
$x_3^2$	4.24	1	4.24	161.46	<0.0001 **
Residual	0.18	7	0.026		
Lack of Fit	0.12	3	0.042	2.82	0.2953
Pure Error	0.059	4	0.015		
Cor Total	20.31	16			

$R^2 = 0.9910$ ;  $R^2_{adj} = 0.9793$ ; CV (Coefficient of Variation) = 3.12%; Adeq precious = 22.97

Note: \*\* and \* indicated significance at 0.01 and 0.05 levels, respectively.

- (2) The regression equation of the consistency coefficient  $Y_2$  of each row after excluding the insignificant indigenous term is:

$$Y_2 = 0.79 - 0.26x_1 + 0.071x_2 + 0.16x_3 + 0.35x_1x_2 - 0.20x_1x_3 + 0.16x_2x_3 + 0.43x_1^2 + 0.33x_2^2 + 0.16x_3^2 \tag{24}$$

Table 5 shows the results of the variance analysis. The consistency coefficient regression model of each row showed that the model was extremely significant ( $p < 0.01$ ), and the mismatch item was not significant ( $p \geq 0.05$ ). The model was effective with determination coefficient  $R^2 = 0.991$ ; the calibration coefficient was 0.981, both were close to 1, and  $CV = 4.88\%$ , Adeq precious = 82.66, indicating that the fitting equation was reliable. Among them, the rotational speed of the metering wheel, the depth of the hole, and the hole's diameter have extremely significant indigenous effects on the equation. The influence order of various factors on the coefficient of variation for consistency of seed quantity in each row  $Y_2$  of each row is the depth of the hole  $x_3$ , the rotational speed of the metering wheel  $x_1$ , and the diameter of the hole  $x_2$ . The Formula (24) shows that the coefficient of variation for consistency of seed quantity in each row  $Y_2$  of each row is a quadratic function with the rotational speed of the metering wheel  $x_1$ , the diameter of the hole  $x_2$ , and the depth of

the hole  $x_3$ , respectively. It shows an optimal group of the rotational speed of the metering wheel, the diameter of the hole, and the depth of the hole to minimize the coefficient of variation for consistency of seed quantity in each row.

**Table 5.** Coefficient of variation for consistency of seed quantity in each row.

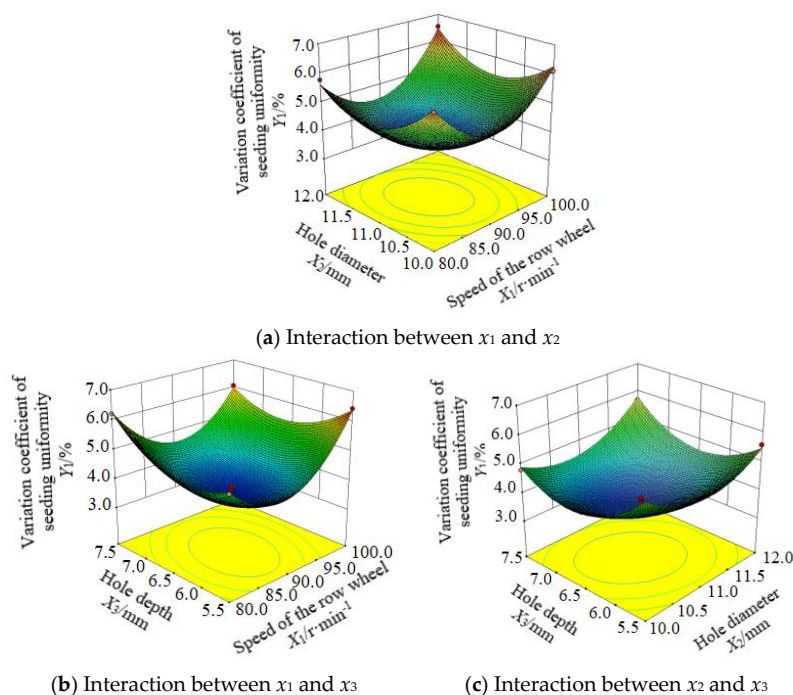
Variance Source	Coefficient of Variation for Consistency of Seed Quantity in Each Row $Y_2/\%$				
	Sum of Square	Degree of Freedom	Mean Square	F Value	p Value
Model	3.05	9	0.34	94.60	<0.0001 **
$x_1$	0.55	1	0.55	154.01	<0.0001 **
$x_2$	0.041	1	0.041	11.35	0.0119 *
$x_3$	0.20	1	0.20	54.57	0.0002 **
$x_1 \times 2$	0.50	1	0.50	140.84	<0.0001 **
$x_1 \times 3$	0.17	1	0.17	46.96	0.0002 **
$x_2 \times 3$	0.11	1	0.11	29.51	0.0010 **
$x_1^2$	0.78	1	0.78	217.76	<0.0001 **
$x_2^2$	0.47	1	0.47	130.25	<0.0001 **
$x_3^2$	0.10	1	0.10	29.27	0.0010 **
Residual	0.025	7	0.0035		
Lack of Fit	0.0033	3	0.0011	0.21	0.8864
Pure Error	0.022	4	0.0054		
Cor Total	3.07	16			

$R^2 = 0.9918$ ;  $R^2_{adj} = 0.9814$ ; CV (Coefficient of Variation) = 4.88%; Adeq precious = 82.66.

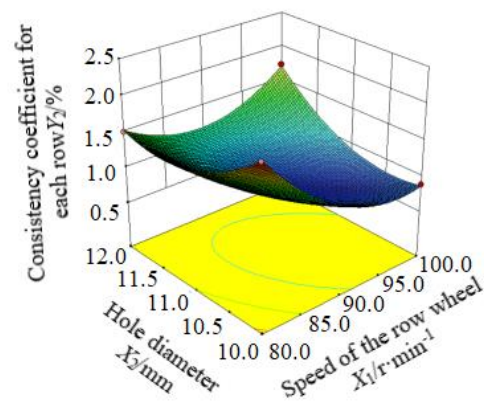
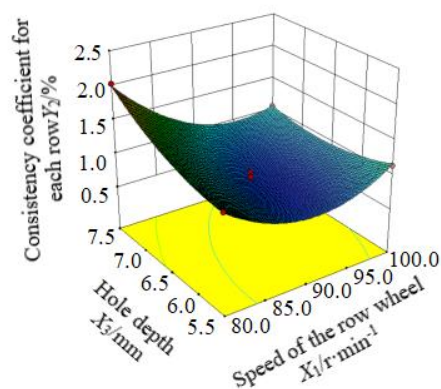
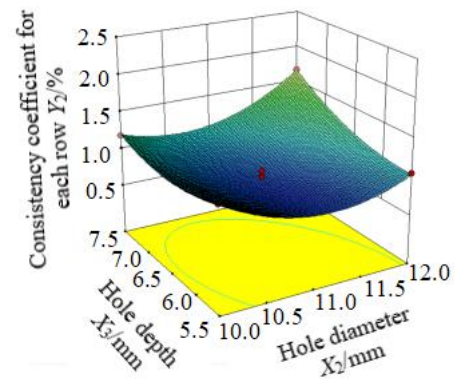
Note: \*\* and \* indicated significance at 0.01 and 0.05 levels.

#### 4.5.2. Effect of Interaction among Factors on Test Indexes

In this study, the variation coefficient of seeding uniformity and coefficient of variation for consistency of seed quantity in each row were used as the evaluation indexes of the seeding performance of self-propelled industrial hemp seeders. Design-Expert software was used for data processing to obtain the response surface of the influence of the interaction between various factors on the evaluation indexes shown in Figures 13 and 14.



**Figure 13.** Response surface of the interaction of factors on the variation coefficient of seeding uniformity.

(a) Interaction between  $x_1$  and  $x_2$ (b) Interaction between  $x_1$  and  $x_3$ (c) Interaction between  $x_2$  and  $x_3$ 

**Figure 14.** Response surface of the interaction of factors on consistency coefficient for each row.

(1) Effect of interaction on variation coefficient of seeding uniformity

As shown in Figure 13a, when the hole depth is 7.5 mm, the interaction between the hole diameter  $x_2$  and the rotation speed  $x_1$  of the metering wheel affects the variation coefficient of seeding uniformity. When the rotation speed  $x_1$  is 90 r/min, the variation coefficient of seeding uniformity first decreases and then increases with the increase in hole diameter  $x_2$ . When the diameter of hole  $x_2$  is 10 mm, the coefficient of variation of seed row uniformity decreases first and then increases with the increase in metering wheel speed  $x_1$ . The slope of the response surface is large, so there is a significant correlation between them. Figure 13b shows the effect of the interaction between hole depth  $x_3$  and rotation speed  $x_1$  on the variation coefficient of seeding uniformity when the diameter of type hole is set at the center level. When the rotation speed  $x_1$  is 90 r/min, the variation coefficient of seeding uniformity decreases first and then increases with the increase in hole depth  $x_3$ . When the hole depth  $x_3$  is 7.5 mm, the variation coefficient of seeding uniformity decreases first. It then decreases with the increase in rotational speed  $x_1$ , and the slope of the response surface is large. The interaction between rotational speed  $x_1$  and hole depth  $x_3$  cannot be ignored.

Figure 13c shows the effect of the interaction between the hole depth  $x_3$  and the hole diameter  $x_2$  on the variation coefficient of seeding uniformity when the rotation speed  $x_1$  is taken as the central level. When the hole diameter  $x_2$  is constant, the variation coefficient of seeding uniformity decreases first and then increases with the increase in hole depth  $x_3$ . When the hole depth  $x_3$  is stable, the variation coefficient of seeding uniformity decreases first and then increases with the increase in hole diameter  $x_2$ . The contour curvature of the response surface is gentle, and the correlation between them is small.



(2) Effect of interaction on the coefficient of variation for consistency of seed quantity in each row

Figure 14a is the effect of the interaction between hole diameter  $x_2$  and the rotation speed  $x_1$  on the coefficient of variation for consistency of seed quantity in each row. When the rotational speed of the metering wheel  $x_1$  is constant, each row's coefficient of displacement consistency coefficient increases with the increase in hole diameter  $x_2$ . When the hole diameter  $x_2$  is constant, the displacement coefficient of variation for consistency of seed quantity in each row decreases first and then increases with the rise of the rotation speed  $x_1$  of the metering wheel.

Figure 14b shows the effect of the interaction between the hole depth  $x_3$  and the rotation speed  $x_1$  on the coefficient of variation for consistency of seed quantity in each row. When the rotational speed of the metering wheel  $x_1$  is constant, the coefficient of variation for consistency of seed quantity in each row decreases with the increase in the hole depth  $x_3$ . When the hole depth  $x_3$  is constant, the displacement coefficient of variation for consistency of seed quantity in each row decreases first and then increases with the increase in the rotation speed  $x_1$  of the metering wheel. Figure 14c shows the influence of the interaction between the hole depth  $x_3$  and the hole diameter  $x_2$  on the coefficient of variation for consistency of seed quantity in each row. When the hole diameter  $x_2$  is constant, the displacement coefficient of variation for consistency of seed quantity in each row decreases first and then increases with the increase in hole depth  $x_3$ . When the hole depth  $x_3$  is constant, the displacement coefficient of variation for consistency of seed quantity in each row decreases first and then increases with the increase in hole diameter  $x_2$ .

4.5.3. The Field Test

To obtain better seeding uniformity of self-propelled industrial hemp seeders under the premise of 57.6~62.4 kg/hm<sup>2</sup>, the optimization parameter optimization module built in the software Design Expert 11.0 is used to solve the problem by extreme value theory. The optimization objective function and constraint conditions are shown in Formula (25). To facilitate the design of the working parameters and structural parameters of the metering wheel, when the operating speed of the machine is 4.7 km/h, the optimal parameters are the rotational speed of the metering wheel  $n = 90.0$  r/min, the diameter of the hole  $d = 10.4$  mm and the depth of the hole  $h = 6.4$  mm, the variation coefficient of the uniformity of the metering is 3.66%. The coefficient of variation for consistency of seed quantity in each row is 0.78%.

$$\begin{cases} \min Y_1(X_1, X_2, X_3) \\ \min Y_2(X_1, X_2, X_3) \\ s.t. \begin{cases} 80.0 \text{ r/min} \leq X_1 \leq 100.0 \text{ r/min} \\ 5.5 \text{ mm} \leq X_2 \leq 7.5 \text{ mm} \\ 10.0 \text{ mm} \leq X_3 \leq 12.0 \text{ mm} \end{cases} \end{cases} \quad (25)$$

In order to verify the reliability of the optimal parameter group and investigate the seeding performance of the self-propelled industrial hemp seeder, a field seeding test was carried out in the National Ramie Storage, Institute of Bast Fiber Crops, Chinese Academy of Agricultural Sciences on 18 April 2021, as shown in Figure 15. According to the horizontal combination of the superior factors in the bench test, the rotation speed of the seed row wheel was adjusted to 90 r/min, the hole diameter was 10.4 mm, and the hole depth was 6.4 mm. The test unit ensured the straight line was forward, and the operating speed of the drill was set to 4.7 km/h to carry out the field test.



**Figure 15.** The field test. (a) Seeder field operation. (b) Growth of industrial hemp.

The experiment took “Long Ma 3” as the seed row object, sowing 3 rows in each stroke with a row spacing of 150 mm. After seedling emergence, according to the distribution of industrial hemp in the field, 5 sections of each row were randomly tested. The verification results are shown in Table 6. The average variation coefficient of actual seeding uniformity is 6.19%, the average coefficient of variation for consistency of seed quantity in each row is 3.44%, and the coefficient is less than 8.0%, which meets the design requirements. The test results are consistent with the optimization results, which are credible.

**Table 6.** Verified results.

Levels	Variation Coefficient of Seeding Uniformity $Y_1/\%$	Coefficient of Variation for Consistency of Seed Quantity in Each Row $Y_2/\%$
1	6.03%	3.58%
2	5.35%	3.29%
3	6.49%	2.80%
4	7.06%	3.71%
5	6.03%	3.82%
Average	6.19%	3.44%

## 5. Conclusions

In this study, the performance test of a self-propelled industrial hemp seed seeder was carried out, and the industrial hemp seed seeder was designed. It is helpful to solve the problem of low efficiency of hemp cultivation in mountainous areas. The main conclusions are as follows:

1. According to the planting mode of industrial hemp for fiber in hilly and mountainous areas, the design of the industrial hemp seed metering device was carried out around the self-propelled industrial hemp seeder. The power chassis system drove the power input seeding and fertilization system to drive the rotation of the metering wheel so that the industrial hemp seeds in the hole of the metering wheel were dropped to the ditch by gravity after passing through the seed protection plate to complete the seeding operation. Through theoretical analysis, the structural parameters and structural parameters of the seed metering wheel are determined.
2. We took the rotation speed of the seeding wheel, the depth of the seeding hole, and the diameter of the seeding hole as the test factors, and the variation coefficient of seed metering uniformity and seed metering quantity as the evaluation indexes. The value range of each factor was determined when the seed metering device met the total seeding quantity of 57.6~62.4 kg/hm<sup>2</sup>. We used the quadratic orthogonal rotating center combination test with three factors and three levels and carried out

a regression analysis on the test results. The test results showed that: the seeding wheel speed had a significant impact on the seeding uniformity and the line displacement consistency coefficient.

3. To optimize the structural and operational parameters of the wheel setter, we used Design-Expert 11.0 for optimization analysis. When the operating speed of the seeder was 4.7 km/h, the speed of the seed row wheel is 90.0 r/min, the diameter of the hole is 10.4 mm, and the depth of the hole is 6.4 mm in the optimal parameter group. At this time, the coefficient of variation of seed row uniformity was 3.66% and the coefficient of consistency of row displacement was 0.78%, both of which were better than the industry standard.
4. In order to verify the practical application effect of the planter, we carried out field experiments on the optimized seeder. The results showed that the average variation coefficient of the actual seeding uniformity was 6.19%. The average coefficient of variation for consistency of seed quantity in each row displacement was 3.44%, which was much less than 8.0%, and the seeding performance was essentially consistent with the optimization results. The self-walking industrial hemp seeder could satisfy the design requirements and effectively improve the cultivation efficiency of fiber industrial hemp in mountainous areas and solve the problem of heavy labor intensity in artificial planting.

**Author Contributions:** Conceptualization, Y.D. and W.X.; methodology, Y.D. and W.X.; software, Y.D. and Y.H.; validation, Y.D.; investigation, W.X. and Y.D.; resources, M.W.; data curation, M.W.; writing—original draft preparation, Y.D. and W.X.; writing—review and editing, W.X. and J.L.; visualization, M.W. and B.Y.; supervision, W.X.; funding acquisition, M.W. and J.L. All authors have read and agreed to the published version of the manuscript.

**Funding:** This research was funded by The science and technology innovation project of Chinese Academy of Agricultural Sciences, grant number “CAAS-ASTIP-21-IBFC07”; “Double first-class” construction project of Hunan Agricultural University, grant number “SYL201802018”; National hemp industry technology system primary processing mechanization post project, grant number “CARS-16-E21”.

**Institutional Review Board Statement:** Not applicable.

**Informed Consent Statement:** Not applicable.

**Data Availability Statement:** All data are presented in this article in the form of figures and tables.

**Conflicts of Interest:** The authors declare no conflict of interest.

## References

1. Manaia, J.P.; Manaia, A.T.; Rodrigues, L. Industrial hemp fibers: An Overview. *Fibers* **2019**, *7*, 106. [[CrossRef](#)]
2. Cherney, J.H.; Small, E. Industrial hemp in north America: Production, Politics and Potential. *Agronomy* **2016**, *6*, 58. [[CrossRef](#)]
3. Xiang, W.; Ma, L.; Liu, J.J.; Yan, B.; Duan, Y.P.; Hu, Y.; Lyu, J.N. Review on technology and equipment of mechanization for industrial hemp in China. *Plant Fiber Sci. China*. **2021**, *43*, 320–332.
4. Wang, Y.F.; Qiu, C.S.; Hao, D.M.; Chen, X.B.; Long, S.H.; Deng, X.; Yu, W.J.; Jia, W.Q. Production status and developmental direction of hemp in China. *Modern Agricul. Sci. Tech.* **2009**, *23*, 84–86.
5. Su, F.F.; Yang, G.; Zheng, Y.G. Industrial hemp cultivation and breeding research on the current situation. *Chin. J. Trad. Chin. Med.* **2022**, *47*, 1190–1195.
6. Lyu, J.N.; Ma, L.; Liu, J.J.; Long, C.H.; Zhou, W. The investigation on the development of industrial hemp and its harvesting machinery of Hei Long Jiang province. *Chin. Hemp. Sci.* **2017**, *39*, 94–102.
7. Jiang, S.; Wang, Q.; Zhong, G.; Tong, Z.; Wang, X.; Xu, J. Brief review of minimum or no-till seeders in china. *Agric. Eng.* **2021**, *3*, 605–621. [[CrossRef](#)]
8. Kamgar, S.; Noei-Khodabadi, F.; Shafaei, S.M. Design, development and field assessment of a controlled seed metering unit to be used in grain drills for direct seeding of wheat. *Inf. Process. Agric.* **2015**, *2*, 169–176. [[CrossRef](#)]
9. Li, H.; Liu, H.; Zhou, J.; Wei, G.; Shi, S.; Zhang, X.; Zhang, R.; Zhu, H.; He, T. Development and first results of a no-till pneumatic seeder for maize precise sowing in huang-huai-hai plain of China. *Agriculture* **2021**, *11*, 1023. [[CrossRef](#)]
10. Wu, M.L.; Guan, C.Y.; Gao, X.Y.; Luo, X. Test on limit turning speed of eccentric round hole-wheel seed meter for rape. *Trans. Chin. Soc. Agric. Engin.* **2010**, *26*, 119–123.

11. Liao, Q.X.; Lei, X.L.; Liao, Y.T.; Ding, Y.; Zhang, Q.; Wang, L. Research progress of precision seeding for rapeseed. *Chin. Soc. Agric. Mach.* **2017**, *48*, 1–16.
12. Yang, L.; Yan, B.X.; Zhang, D.X.; Zhang, T.; Wang, Y.; Cui, T. Research progress on precision planting technology of maize. *Chin. Soc. Agric. Mach.* **2016**, *47*, 38–48.
13. Liao, Y.T.; Wang, L.; Liao, Q.X. Design and test of an inside-filling pneumatic precision centralized seed-metering device for rapeseed. *Int. J. Agric. Biol. Eng.* **2017**, *10*, 56–62.
14. Li, H.C.; Gao, F.; Zhao, S.; Liu, W. Domestic and overseas research status and development trend of precision seed metering device. *J. Chin. Agric. Mech.* **2014**, *35*, 12–16, 56. [[CrossRef](#)]
15. Chen, Y.; Cheng, Y.; Chen, J.; Zheng, Z. Design and experiment of the buckwheat hill-drop planter hole forming device. *Agriculture* **2021**, *11*, 1085. [[CrossRef](#)]
16. Sun, X.; Li, H.; Qi, X.; Nyambura, S.M.; Yin, J.; Ma, Y.; Wang, J. Performance parameters optimization of a three-row pneumatic precision metering device for brassica chinensis. *Agronomy* **2022**, *12*, 1011. [[CrossRef](#)]
17. Wang, B.; Na, Y.; Liu, J.; Wang, Z. Design and evaluation of vacuum central drum seed metering device. *Appl. Sci.* **2022**, *12*, 2159. [[CrossRef](#)]
18. Liu, Y.; Lin, J.; Li, B.; Ma, T. Design and experiment of horizontal disc seed metering device for maize seeder. *Trans. Chin. Soc. Agric. Eng.* **2017**, *33*, 37–46.
19. Guler, I.E. Effects of flute diameter, fluted roll length, and speed on alfalfa seed flow. *Appl. Eng. Agric.* **2005**, *21*, 5–7. [[CrossRef](#)]
20. Singh, R.C.; Singh, G.; Saraswat, D.C. Optimisation of design and operational parameters of a pneumatic seed metering device for planting cottonseeds. *Biost. Eng.* **2005**, *92*, 429–438. [[CrossRef](#)]
21. Yazgi, A.; Degirmencioglu, A. Measurement of seed spacing uniformity performance of a precision metering unit as function of the number of holes on vacuum plate. *Measurement* **2014**, *56*, 128–135. [[CrossRef](#)]
22. Singh, T.; Mane, D. Development and laboratory performance of an electronically controlled metering mechanism for okra seed. *Agric. Mech. Asia Afr. Lat. Am.* **2011**, *42*, 63–69.
23. Wang, S.W.; Song, Y.Z. *Hemp Crop Production Machinery*, 1st ed.; China Agriculture Press: Beijing, China, 1997; pp. 258–267.
24. Wang, J.W.; Tang, H.; Guan, R.; Li, X.; Bai, C.H.; Tian, L.Q. Design and experiment on clamping static and dynamic finger-spoon maize precision seed metering device. *Chin. Soc. Agric. Mach.* **2017**, *48*, 48–57.
25. Yi, S.J.; Chen, T.; Li, Y.F.; Tao, G.; Mao, X. Design and test of millet hill-drop seed-metering device with combination of positive-negative pressure and hole wheel. *Chin. Soc. Agric. Mach.* **2021**, *52*, 83–94.
26. Zhu, D.Q.; Li, L.L.; Wen, S.C.; Zhang, S.; Jiang, R.; Wu, L.Q. Numerical simulation and experiment on seeding performance of slide hole-wheel precision seed-metering device for rice. *Trans. Chin. Soc. Agric. Eng.* **2018**, *34*, 17–26.
27. China Academy of Agricultural Mechanization Sciences. *Agricultural Machinery Design Manual, Upper*; China Agriculture Science Technology Press: Beijing, China, 2007; pp. 347–348.
28. Xiong, D.Y.; Wu, M.; Xie, W.; Liu, R.; Luo, H. Design and experimental study of the general mechanical pneumatic combined seed metering device. *Appl. Sci.* **2021**, *11*, 7223. [[CrossRef](#)]
29. Lian, Z.; Wang, J.; Yang, Z.; Shang, S.Q. Development of plot-sowing mechanization in China. *Trans. Chin. Soc. Agric. Eng.* **2012**, *28*, 140–145.
30. Zhang, S.; Xia, J.F.; Zhou, Y.; Zhai, J. Design and experiment of pneumatic cylinder-type precision direct seed-metering device for rice. *Trans. Chin. Soc. Agric. Engin.* **2015**, *31*, 11–19.
31. Ding, L.; Yang, L.; Zhang, D.X.; Gui, T.; Zhang, K.; Zhong, X. Effect of seed adsorption posture of corn air-suction metering device on seed feeding performance. *Chin. Soc. Agric. Mach.* **2021**, *52*, 40–50.
32. Su, W.; Chen, Z.W.; Lai, Q.H.; Jia, G.X.; Lyu, Q.; Tian, B.N. Design and test of wheel-spoon type precision seed-metering device for Chinese herbal medicine *Pinellia ternata*. *Chin. Soc. Agric. Mach.* **2022**, 1–15.
33. Jiang, M.; Liu, C.L.; Wei, D.; Du, X.; Cai, P.; Song, J. Design and test of wide seedling strip wheat precision planter. *Chin. Soc. Agric. Mach.* **2019**, *50*, 53–62.
34. Lai, Q.H.; Jia, G.X.; Su, W.; Hong, F.; Zhao, J. Design and test of ginseng precision special-hole type seed-metering device with convex hull. *Chin. Soc. Agric. Mach.* **2021**, *51*, 60–71.
35. Zhang, S.; Li, Y.; Wang, H.Y.; Liao, J.; Li, Z.; Zhu, D. Design and Experiment of U-shaped Cavity Type Precision Hill-drop Seed-metering Device for Rice. *Chin. Soc. Agric. Mach.* **2020**, *51*, 98–108.
36. Song, Y. *Summary of Agricultural Mechanization Standards*, 1st ed.; China Agriculture Press: Beijing, China, 2013; pp. 315–316.